

Research Article: New Research | Disorders of the Nervous System

# Affection of Motor Network Regions by Tau Pathology Across the Alzheimer's Disease Spectrum

https://doi.org/10.1523/ENEURO.0242-23.2023

Received: 11 July 2023 Revised: 8 September 2023 Accepted: 19 September 2023

Copyright © 2023 Bischof et al.

This is an open-access article distributed under the terms of the Creative Commons Attribution 4.0 International license, which permits unrestricted use, distribution and reproduction in any medium provided that the original work is properly attributed.

This Early Release article has been peer reviewed and accepted, but has not been through the composition and copyediting processes. The final version may differ slightly in style or formatting and will contain links to any extended data.

**Alerts:** Sign up at www.eneuro.org/alerts to receive customized email alerts when the fully formatted version of this article is published.

Running Title: Tau pathology in higher-order motor regions

- 1 Title:
- 2 Affection of motor network regions by tau pathology across the Alzheimer's Disease
- 3 spectrum.
- 4 **Authors:**
- 5 Gérard N Bischof <sup>1,2</sup>, Elena Jaeger<sup>1</sup>, Kathrin Giehl <sup>1,2</sup>, Merle C Hönig <sup>1,2</sup>, and for the
- 6 Alzheimer's Disease Neuroimaging Initiative\*, Peter H. Weiss<sup>3,4</sup> & Alexander Drzezga<sup>1,2,6</sup>
- 7 \* Data used in preparation of this article were obtained from the Alzheimer's disease
- 8 Neuroimaging Initiative (ADNI) database (http://adni.loni.usc.edu). Thus, the investigators
- 9 within the ADNI contributed to the design and implementation of ADNI and/or provided data,
- but did not participate in this analysis or the writing of this report. A complete listing of ADNI
- investigators can be found at http://adni.loni.usc.edu/wpcontent/uploads/how\_to\_apply
- 12 /ADNI\_Acknowledgement\_List.pdf/.

## 14 Affiliations:

13

- <sup>1</sup> University of Cologne, Faculty of Medicine and University Hospital of Cologne, Department
- of Nuclear Medicine, Cologne, Germany
- <sup>2</sup> Research Center Juelich, Institute for Neuroscience and Medicine II, Molecular Organization
- of the Brain, Juelich, Germany
- <sup>3</sup> Research Center Juelich, Institute for Neuroscience and Medicine III, Cognitive Neuroscience,
- 20 Juelich, Germany
- <sup>5</sup> University of Cologne, Faculty of Medicine and University Hospital of Cologne, Department
- of Neurology, Cologne, Germany
- <sup>6</sup> German Center for Neurodegenerative Diseases, Bonn/Cologne, Germany

**Corresponding Author:** Dr. Gérard N Bischof, University of Cologne, Faculty of Medicine and University Hospital of Cologne, Department of Nuclear Medicine, Multimodal Neuroimaging Group, Kerpener Straße 62, 50937 Cologne, Germany E-mail: gerard.bischof@uk-koeln.de phone: +49 221 478 86621 Number of pages: 25 Number of figures, tables: 3; 3 . (sepa Number of words for abstract, introduction, and discussion (separately): 250; 531; 1446 

## Abstract

50

51

52

53

54

55

56

57

58

59

60

61

62

63

64

65

66

67

68

69

70

Stereotypical isocortical tau protein pathology along the Braak-Stages has been described as an instigator of neurodegeneration in Alzheimer's Disease (AD). Less is known about tau pathology in motor regions, although higher-order motor deficits such as praxis dysfunction are part of the clinical description. Here, we examined how tau pathology in cytoarchitectonically mapped regions of the primary and higher-order motor network in comparison to primary visual and sensory regions varies across the clinical spectrum of AD. We analyzed tau PET scans from the ADNI-cohort in patients with mild cognitive impairment (MCI; N=84) and dementia of the Alzheimer's Disease type (DAD; N=25). Additionally, an amyloid-negative sample of healthy older individuals (HC; N=26) were included. Standarduptake ratio values (SUVR) were extracted in native space from the left and the right hemispheres. A repeated measurement analysis of variance was conducted to assess the effect of diagnostic disease category on tau pathology in the individual motor regions, controlling for age. We observed that tau pathology varies as a function of diagnostic category in predominantly higher motor regions (i.e., supplementary motor area, superior parietal lobe, angular gyrus and dorsal premotor cortex) compared to primary visual, sensory and motor regions. Indeed, tau in higher-order motor regions was significantly associated with decline in cognitive function. Together, these results expand our knowledge on the in vivo pattern of tau pathology in AD and suggest that higher motor regions are not spared from tau aggregation in the course of disease, potentially contributing to the symptomatic appearance of the disease.

71

72

73

74

75

76

77

## **Significance Statement:**

The presented data show relevant tau pathology in higher-order motor regions of patients with mild cognitive impairment (MCI) and dementia of the Alzheimer's Disease type (DAD), in a set of regions often neglected in the previous literature. Tau accumulation in higher-order motor regions was associated with clinical disease severity and increased cognitive dysfunction. These findings suggest that the concerted vulnerability of motor regions to tau pathology may contribute to motor/ praxis dysfunction observed in Alzheimer's Disease.

79

78

80 81 **Keywords**: Alzheimer's disease, mild cognitive impairment, regional tau burden, motor

regions, positron emission tomography

#### 1. INTRODUCTION

Alzheimer's disease (AD) pathology is characterized by the build-up of senile plaques composed of beta-amyloid in the extracellular space and neurofibrillary tangles composed of tau proteins in the intracellular space. Beta-amyloid generally appears first in the neocortex, and then spreads to the allocortex and subcortical regions as the disease advances (Thal et al., 2002; Grothe et al., 2017). In contrast, tau has been described by a stereotypical spreading pattern starting in transenthorinal regions, progressing to temporal allocortex, followed by parietal and occipital high-order association areas and prefrontal regions, before spreading to unimodal sensory and premotor areas (Braak and Braak, 1995; Braak et al., 2011). *In vivo* imaging using positron emission tomography (PET) of AD pathology has provided general correspondence for the histopathological distribution of both protein pathologies (Thal et al., 2002; Schöll et al., 2016; Schwarz et al., 2016; Bischof et al., 2017; Grothe et al., 2017; Jack et al., 2018), whereas the regional accumulation of tangle pathology has been shown to be stronger related to the clinical symptoms compared to beta-amyloid plaques (Dronse et al., 2016; Ossenkoppele et al., 2016).

However, *in vivo* imaging offers the novel opportunity to evaluate if tau pathology is present in regions, which are often neglected in the staging scheme stated by histopathological studies. Indeed, for example, regions of the lateral occipital cortex were associated with tau accumulation in histopathological studies in late disease only, but were found in mild and moderate stages of the disease (Schwarz et al., 2016) using *in vivo* PET. Likewise, regions of the motor system have gained little attention in histopathological studies. For instance,

histopathological studies revealed beta-amyloid accumulation in primary motor regions in Thal stage 4 and 5 that preceded subcortical burden of beta amyloid in regions of the hippocampus (Murray et al., 2015). Similarly, tau pathology has been described in sensorimotor cortex only in late isocortical disease stages (Schwarz et al., 2016). Yet, a systematic *in vivo* study on the distribution of tau pathology in regions of the motor network is missing, although it is feasible that tau in motor regions may contribute to the clinical symptomatology of AD.

Notably, there is a great deal of clinical interest in the evaluation of motor symptoms, as apraxia has been reported in patients with a clinical diagnosis of dementia of the Alzheimer's disease type (DAD) with up to 32 % (Ozkan et al., 2013) and has been recognized as a symptom category that can differentiate variants of dementia based on the specific apraxia profile (Johnen et al., 2018). It is widely unknown, however, which aspects of the pathophysiological disease cascade contributes to motor deficits in AD. Specifically, it has yet to be determined whether significant tau pathology can be found in motor regions of DAD patients. Here, we probed these questions by first quantifying the *in vivo* tau deposition in motor regions in patients clinically diagnosed with mild cognitive impairment (MCI) and DAD patients (compared to healthy older participants). Secondly, we evaluated if the level of tau deposition in motor regions (compared to control regions) was associated with disease stage or general cognitive dysfunction.

## 2. Material and Methods

#### 2.1 Participants

Data used for this study were derived from the Alzheimer's Disease Neuroimaging Initiative (ADNI) (<a href="http://adni.loni.usc.edu/">http://adni.loni.usc.edu/</a>). Screening criteria were: 1) Information on amyloid status, 2) Availability of a 18F-AV1451 scan, 3) Available MRI-Scan within an appropriate time window around 18F-AV1451 scan acquisition with the longest acceptable difference

between MRI and 18F-AV1451 being six months (median time difference = 14 days with standard deviation (SD) = 38.17 days).

The patients with clinical dementia due to AD met the National Institute of Neurological and Communicative Disorders and Stroke–Alzheimer's Disease and Related Disorders Association criteria for probable AD (McKhann et al., 1984). Briefly, patients with DAD had progressive deterioration of memory and other cognitive domains, objectively evaluated in a clinical exam in the absence of another systemic, psychiatric or neurological disease that could potentially explain dementia symptoms. Activities of daily living (ADL) were impaired. Patients with MCI reported subjective memory concern either autonomously or via an informant or clinician and showed an objective cognitive impairment defined by education-adjusted scores with 1.5 SDs below the normative mean on delayed recall of Wechsler-Memory-Scale Story A. ADL were essentially preserved, and no signs of dementia existed (Petersen et al., 2010). Healthy controls (HC) in this sample showed no signs of depression, did not fulfill criteria for MCI or DAD and were amyloid negative based on PET or CSF information derived from ADNI (https://adni.loni.usc.edu/methods/) closest to the tau PET scans.

## 2.2 Experimental Design and Statistical Analyses

#### 2.3 Neuropsychological tests to assess global cognitive performance

All participants underwent neuropsychological testing using the Alzheimer's Disease Assessment Scale-Cognitive Subscale (ADAS-Cog-13). The cognitive subscale includes thirteen self-completed or observer-based assessments evaluating the cognitive domains of memory, language, attention, and concentration. For our analysis, we calculated the global performance score on the ADAS-Cog-13. Of note, severity in cognitive decline is quantified by higher values on the ADAS-subscale culminating in higher scores in more progressed patients.

Additionally, neuropsychological test scores of the Mini-Mental Examination Test (MMSE) were used to describe the status of global cognitive function of each participant in the groups.

## 2.4 Positron Emission Tomography (PET) Acquisition

18F-AV1451 PET imaging was acquired using a static imaging protocol 75 minutes post-injection of ~370 MBq (10mCi) of the tracer. Participants were scanned for 30 minutes and six 5-minutes frames were recorded. Body weight and injected-dose corrected frames were co-registered to one another to reduce motion effects and the five frames were averaged to a single 30 minutes PET image set for each participant.

#### 2.5 Magnetic-Resonance Imaging (MRI) Acquisition

Structural Magnet Resonance Imaging (MRI) datasets acquired closest to the date of the 18F-AV1451 PET scan were downloaded from the ADNI database for co-registration with the 18F-AV1451 PET scan.

Structural MRIs were acquired on 3 T scanners using a high-resolution T1-weighted magnetization prepared rapid gradient echo (MPRAGE) sequence with the following parameters: TR = 2300, TE = minimum full echo, TI = 900,  $FOV = 208 \times 240 \times 256$  mm, and  $1 \times 1 \times 1$  mm resolution.

## 2.6 Image Preprocessing

Individual 18F-AV1451 PET scans were co-registered to the individual anatomical MPRAGE scan. Each MPRAGE scan was segmented into three tissue classes (i.e., gray matter, white matter, and cerebral spinal fluid (CSF)) using the segmentation function of the Partial Volume Effects correction in brain PET toolbox implemented in SPM 12 (PETPVE12; (Gonzalez-Escamilla et al., 2017). Importantly, for each individual MPRAGE scan deformation fields for each individual were derived from diffeomorphic Anatomical Registration Through

Exponentiated Lie Algebra (DARTEL) registration to the reference template (IXI550\_MNI152.nii) implemented in PETPVE12. Regions of interests (ROI) were overlaid on co-registered 18F-AV1451 PET scans using the deformation field of the individual native PET-space.

#### 2.7 Region of Interests Selection

SPM Anatomy Toolbox Version 3 implemented in SPM 12 (https://www.fz-juelich.de/en/inm/inm-7/resources/jubrain-anatomy-toolbox) was used to create an anatomical mask of the left and right cortical and primary motor regions associated with main motor function and of primary visual, primary sensory as control regions. As there are some known lateralization differences in motor regions (Mutha et al., 2012), we decided to separate the regions by hemisphere. Table 1 lists the derived ROIs and their respective nomenclature in the Julich Brain cytoarchitectonic atlas (Eickhoff et al., 2005) and a display of the examined regions is depicted in Figure 1.

## 2.8 Standard Uptake Value Ratio Quantification

Region-specific standard uptake values (SUV) were extracted from 18F-AV1451 PET scans and from the vermis reference region for each individual subject in native space (*see* Table 1). To create standardized uptake value ratios (SUVRs), region-specific SUVs were divided by SUVs extracted from the vermis reference region, known to show little specific binding. Of note, the vermis was selected as a reference region due to its lack of involvement in limb motor function, unlike other subregions of the cerebellum (Klein et al., 2016).

## 2.9 Statistical Analysis

Potential differences in continuous demographic variables (*see* Table 2) were statistically assessed using univariate analyses of variance (ANOVAs) with group as a factor, whereas categorical variables were examined by Chi-Square ( $X^2$ ) to assess group specific differences in the frequency distribution. The significance thresholds for these descriptive analyses were set at p < .05.

To evaluate potential differences between groups across the regions known to underlie motor function, we statistically modelled a repeated measurement ANOVA with group as a between-subject factor and age as a covariate. Within subject-factors were hemisphere (left and right) and region (seven primary and higher-order motor regions of interest and two control regions). Potential interaction effects of the factors group and region were then explored for each region by a one-way ANOVA with the between subject factor group. If a significant main effect of group was detected for a given region by the one-way ANOVA, planned post-hoc comparisons were executed to further detail the potential source of the group differences in that region. This allowed us to significantly reduce the number of planned comparisons, despite our hypothesis driven ROI approach. Significance threshold was set at p <0.05.

Supportive evidence for the contribution of tau pathology in anatomical motor regions towards disease severity was evaluated by partial correlation analyses, quantifying the relationship of ADAS-Cog-13 with the tau signal in the respective praxis regions, controlling for diagnostic group and age. Confidence-Intervals for correlation coefficients were calculated using a bootstrap procedure (1000 repetitions) implemented in SPSS v27. All other statistical analyses were performed in SPSS v27 as well.

#### 3. RESULTS

A total of N=135 subjects were included in the analysis. Demographic information on these subjects is summarized in Table 2. Age and MMSE were significantly different among

the groups  $(F_{(Age)}(2,132)=6.515, p=.002; F_{(MMSE)}(2,132)=68.276, p<.001)$ , whereas APOE epsilon 4-allele carrier status and sex distribution were not  $(X^2_{(APOE)}(2,N=135)=7.5, X^2_{(Sex)}(2,N=135)=1.3 p>.05)$ . Due to the group differences in age, age was entered as a covariate in subsequent analysis.

In the repeated measurement ANOVA, we identified a significant Region  $\times$  Group interaction ( $F_{(Region \times Group)}$ ) (2,132) =3.84, p <.024), while none of the remaining main effects or interactive effects reached significance (for details see Table 3). Since neither an interaction nor a main effect of hemisphere was detected, we subsequently averaged SUVR values across the left and the right hemisphere in each region. Further interrogation of the Region  $\times$  Group interaction using one-way ANOVAs with the between-subject factor group for each of the nine regions, revealed that four of the nine regions (i.e., the supplementary motor area (p =.011), the angular gyrus (p = .027), the superior parietal lobe (p = .027), and the dorsal premotor cortex (p =.027)) showed a significant main effect of group, while the other five regions did not (see Table 4). We further analyzed the group differences in the four regions using post-hoc comparisons. Interestingly, in all of these regions the pattern of differences across the groups was similar (see Figure 2 and Figure S1). Specifically, the four higher-order motor regions were characterized by higher tau SUVRs in DAD patients compared to both HC and MCI patients. The results are summarized in Table 5.

Although Area MT/V5 (p <.075) and the supramarginal gyrus (p <.083) showed trend significant group effects only, a similar pattern was observed in these two regions. Albeit not significant, DAD patients had higher tau SUVRs in area MT/V5 and the supramarginal gyrus than MCI patients and HC (see Figure 2, and Figure S1). Importantly, none of the primary regions for motor, sensory or visual processing showed a significant group effect. Moreover, we observed relatively low tracer retention in these three regions (see Figure 2). These results confirm the regional specificity of tau pathology in higher-order motor regions, whereas

primary regions in DAD and MCI patients show negligent levels of tau burden, which are indistinguishable from HC.

To evaluate the potential impact of *in vivo* tau pathology in (higher-order) motor regions on general cognitive dysfunction, we examined the partial correlation between ADAS-Cog-13 and tau SUVR in those motor regions that displayed a significant group effect (i.e., SMA, angular gyrus, superior parietal lobe and dorsal premotor cortex). Partial correlations were corrected by age and group. Indeed, we found moderate, but significant positive correlation coefficients of tau SUVR and increases in ADAS-Cog-13 across the cohort (see Table 5, and Figure 2). Specifically, SMA showed the strongest correlation (r = .251), followed by the angular gyrus (r = .248) and superior parietal lobe and dorsal premotor cortex with the smallest correlation coefficients (r = .232 and r = .208)

#### 4. DISCUSSION

The goal of the study was to examine if relevant *in vivo* tau pathology in prodromal and clinical stages of AD is present in regions of the motor network. We chose cytoarchitectonically parcellated regions of the Juelich-Brain Atlas to allow for distinct and accurate anatomical mapping of motor regions. The Juelich-Brain Atlas is advantages due to its precision and integration of individual variations of stereotaxic space (Amunts et al., 2020) including the core regions of the motor network. We found that increased tau pathology in clinical stages of AD was most pronounced in supplementary motor area, angular gyrus, superior parietal regions and dorsal premotor cortex, whereas trend significant effects were observed for movement-related area MT/V5 and supramarginal gyrus. Importantly, all primary regions, including primary motor, primary sensory and primary visual regions did not show significant alterations as a function of clinical diagnosis of AD. For the higher motor regions showing a significant group

effect, we identified a significant association of general cognitive dysfunction and increases in tau pathology, irrespective of diagnostic group.

Histopathological studies have suggested that early stages of neurofibrillary tangle protein inclusions are present in transenthorinal regions (Braak I-II) prior to the involvement of limbic regions (Braak III-IV) and finally isocortical regions (V-VI), suggesting an area-specific distribution pattern rather than a random occurrence of protein-pathology (Braak and Braak, 1995). With regard to the higher-order motor regions examined here, the majority of regions (i.e., supramarginal gyrus, superior parietal lobe, angular gyrus, premotor areas) have been described to constitute Braak V, whereas regions such as Area MT/V5 and primary sensory and motor neocortex are thought to be part of Braak VI. This is in correspondence to the presented findings here, as elevated tau pathology in higher-order motor regions (i.e., regions included in Braak V) were most visible in the clinical disease stages of DAD followed by prodromal stages of AD compared to healthy controls. Additionally, no significant group differences in primary regions were observed indicating the lack of relevant tau pathology in these regions which confirms the stereotypical pattern of tau in histopathological data.

It is important to note that the driving concept of the histopathological approaches taken by neuropathologist was to describe the anatomical extent of the disease, not primarily the intensity or concentration of the protein inclusions observed (Del Tredici and Braak, 2020). *In vivo* PET imaging of protein pathology can now broaden the scope of our disease understanding by including both extent and intensity and temporal course/symptom correlation to inform on the disease processes. The observed increased uptake pattern in late-stage disease regions can alternatively be explained by different maturity states of tau protein pathology that are detected with 18F- AV1451. Specifically, it is possible that pre-tangle pathology is evolving in higher-order motor regions, as it has been shown that 18F- AV1451 has a higher affinity to pre-tangle

formation of tau, which may be the source of signal we observed here (Braak et al., 2011; Wren et al., 2018).

295

296

297

298

299

300

301

302

303

304

305

306

307

308

309

310

311

312

313

314

315

316

317

318

319

From a motor systems perspective our data provide in vivo evidence for a particular involvement of higher motor regions in the spreading of tau pathology with symptomatic disease progression, which is a novel finding. Lesion studies, mainly performed in stroke patients, indicate that cognitive-motor processes are organized in dorso-dorsal, ventro-dorsal and ventral processing streams (Martin et al., 2017). Our results suggest that particular the dorso-dorsal stream (e.g., dorsal premotor cortex, superior parietal cortex) and part of the ventro-dorsal processing stream (e.g., angular gyrus) are affected by tau pathology in AD. Indeed, major higher-order regions of the motor system spanning from motor planning (angular gyrus) to initiation of internally (e.g., SMA) or externally (e.g., premotor cortex) triggered movements show a significant correlation of increased tau pathology with increasing clinical disease severity. These findings indicate that the motor system is not spared from aggregation of tau pathology even in relatively early stages of disease. It is important to note, that some of the investigated regions have been shown to subserve additional function, such as working memory processing or distributing attentional demands or semantic processing such as the superior parietal lobule or the angular gyrus (Horwitz et al., 1998; Alahmadi, 2021). Given that such functions become gradually impaired with clinical disease severity, it is feasible that tau pathology in these particular regions may impair cognitive processes beyond motor function alone. The distinctiveness and importance of the shown vulnerability of motor regions to the pathophysiological build-up of tau pathology is, however, well represented in the supplementary motor area, a region strictly responsible for motor function (Tanji, 1994; Tanji and Shima, 1996; Côté et al., 2020; Rahimpour et al., 2022).

The consequences of these motor-associated tau aggregates with regard to potential impairment of higher-order motor-cognitive functions are yet unknown, as specific praxis

functions were not examined in this cohort. However, accumulating evidence suggests that specific praxis functions in AD are impaired (Johnen et al., 2015; Yliranta et al., 2023b). Interestingly, some studies suggest that limb apraxia and verbal memory may indeed improve differential diagnosis of DAD compared to other psychiatric etiologies of dementia (Yliranta et al., 2023a). The current study suggests that the potential effects of tau deposition in motor areas on specific motor functions should be further examined. For this reason, our group is currently investigating in a prospective trial, if the clinical symptomatology of praxis dysfunction in DAD is associated with elevated tau pathology in regions subserving higher-order motor function. This may add evidence to the established observation of a close link between the dominant clinical symptoms and the peak regions of the most elevated tau pathology in both typical and atypical AD (Dronse et al., 2016; Ossenkoppele et al., 2016; Bejanin et al., 2017; Bischof et al., 2017). Such imaging-based approaches may also allow to examine *in vivo*, why praxis dysfunction appears to be a later symptom in the sporadic disease cascade only, whereas in early-onset disease cases it has been suggested to be an early behavioral symptom (Yliranta et al., 2023b).

A recent observation which has elucidated our understanding of AD heterogeneity is the presence of endophenotypes based on tau PET scans of 18F-AV1451(Vogel et al., 2021). Briefly, the authors observed several subgroups of tau deposition patterns: a tau pattern most accurately described by elevated limbic tangle deposition (S1: 33 % of the AD sample), a predominant posterior occipital and gradually anterior expanding type (S3: 30 %), a hemispheric dominant temporo-parietal phenotype (S4: 19 %) and, finally, a medial-temporal sparing phenotype, with dominantly parietal lobe involvement (S2: 18 %). Importantly, the investigated phenotypes were characterized by different disease onsets (e.g., S1 and S3 late disease onset), and clinical presentation (e.g., S3 visuospatial impairment, S2: dysexecutive impairment, S4 multi-domain impairment) and disease progression (e.g., S3: slow progressing,

S4: fast progressing). Overall, these data suggest that differential spatial patterns of tau pathology can influence disease trajectories. It will be interesting to further investigate if clinical profiles of praxis dysfunction align with differential patterns of tau deposition in higher-order motor regions and if apraxia could be an additional feature that complements the clinical characteristics of the described tau PET endophenotypes.

Finally, we observed that increased tau deposition in higher-order motor regions was associated with general cognitive dysfunction. Although the correlation coefficients were moderate in size, they provide support for the idea that tau pathology in higher-order motor regions contributes to the cognitive decline in patients with Alzheimer's pathology, over and above the clinically defined diagnostic group.

Some limitations of our current approach should be acknowledged. First of all, although we detected elevated tau pathology in higher-order motor regions, the clinical relevance to the commonly observed praxis deficits in AD could not be interrogated due to the lack of detailed characterization of praxis function in this cohort. Additionally, only cross-sectional inferences on the potential group differences of tau pathology in motor regions can be drawn from this study. It would be interesting to examine how tau pathology in motor regions advances in individuals who progress along on the continuum of AD and how this is associated with accompanying deterioration of cognitive function in the prodromal and the advanced stages of DAD.

A drawback of the tau tracer 18F-AV1451 is the limited ability to accurately measure tau pathology in basal ganglia due to the concomitant non-tau-specific binding, presumably to MAO-A and MAO-B in this brain region (Bischof et al., 2017; Leuzy et al., 2019; Bischof, 2022). The basal ganglia are, however, instrumental for motor control and other next-generation tracers void of non-tau-specific target binding in basal ganglia, may be better suited for further assessment of tau-specific basal ganglia uptake in a motor-centered regional analysis.

In sum, we investigated patterns of elevated tau pathology in motor regions in a large sample of patients with MCI and DAD and observed significant increases of tau pathology in higher-order motor processing regions as compared to HC. Importantly, the level of tau pathology in the investigated pathways was associated with decreases in cognitive function. This indicates a clinicopathological link between tau in motor-cognitive areas, and advances our knowledge beyond the known relationship of tau patterns in medial temporal regions and memory in AD.

## Acknowledgements

AD, GNB, EJ, MH and PHW are funded by the Deutsche Forschungsgemeinschaft - Project-ID 431549029 - SFB 1451. GNB received funding from Alzheimer Forschung Initiative e.V., Germany (AFI K1707). In addition, this study was supported by the German Research Foundation (DFG, DR 445/9-1). Data collection and sharing for this project was funded by the Alzheimer's Disease Neuroimaging Initiative (ADNI) (National Institutes of Health Grant U01 AG024904) and DOD ADNI (Department of Defense award number W81XWH-12-2-0012).

#### **Funding**

ADNI is funded by the National Institute on Aging, the National Institute of
Biomedical Imaging and Bioengineering, and through generous contributions from the
following: AbbVie, Alzheimer's Association; Alzheimer's Drug Discovery Foundation;
Araclon Biotech; BioClinica, Inc.; Biogen; Bristol-Myers Squibb Company; CereSpir, Inc.;
Cogstate; Eisai Inc.; Elan Pharmaceuticals, Inc.; Eli Lilly and Company; EuroImmun; F.
Hoffmann-La Roche Ltd and its affiliated company Genentech, Inc.; Fujirebio; GE
Healthcare; IXICO Ltd.; Janssen Alzheimer Immunotherapy Research & Development, LLC.;
Johnson & Johnson Pharmaceutical Research & Development LLC.; Lumosity; Lundbeck;

Merck & Co., Inc.; Meso Scale Diagnostics, LLC.; NeuroRx Research; Neurotrack

Technologies; Novartis Pharmaceuticals Corporation; Pfizer Inc.; Piramal Imaging; Servier;

Takeda Pharmaceutical Company; and Transition Therapeutics. The Canadian Institutes of

Health Research is providing funds to support ADNI clinical sites in Canada. Private sector

contributions are facilitated by the Foundation for the National Institutes of Health

(www.fnih.org). The grantee organization is the Northern California Institute for Research

and Education, and the study is coordinated by the Alzheimer's Therapeutic Research Institute

at the University of Southern California. ADNI data are disseminated by the Laboratory for

Neuro Imaging at the University of Southern California.

## **Competing Interests**

No competing interest declared.

#### **Author Contributions**

GNB, EJ, KG, MH, PHW, AD designed and developed the concept of the study; ADNI was responsible for the data acquisition; GNB, EJ, KG, PHW, AD assisted in interpretation of data for the article; GNB, PHW, AD drafted the article and GNB, EJ, KG; MH, PHW, and AD revised it critically for important intellectual content.

Anatomical	Region	Definition		
Networks/Regions		Jul-Brain Areas		
Primary Regions				
	Primary Motor	4a, 4p		
	Primary Sensory (S1)	1, 2, 3a, 3b		
	Primary Visual	HOc1		
Dorso-Dorsal Network		150		
	Dorsal premotor cortex	6d1, 6d2, 6d3		
	Superior parietal lobe	5ci, 5l, 5m 7a, 7m, 7p, 7pc		
Common Network		0		
	Angular gyrus	PGa, PGp		
	Lateral occipital cortex/ extra-striate body area	V5		
Supramarginal Gyrus	SMG	PFcm, PFm, PFop, PFt		
Supplementary Motor Area	SMA	6mc, 6mr		

Table 1 Cytoarchitectonically mapped regions of the motor network and the corresponding Broadman Area in the Julich-Brain Atlas. Additionally regions were categorized based on the spatial placement in the motor networks.

4	3	6

		HC (N=26)	MCI+ (N=84)	DAD+ (N=25)
438	Age	73.53 (8.1)	68.61 (5.4)	68.68 (6.3)
439	Sex (% male)	53	56	68
	MMSE	28.7 (1.5)	27.7 (2.0)	22.6 (2.7)
440	APOE (% carrier)	23 %	23%	28 %

 Table 2 Demographic data on included cohort. Data are presented as mean (SD) for continuous variables and percentage for categorical variables. Abbreviations: DAD, Dementia of the Alzheimer's disease type, APOE4, Apolipoprotein E4; HC, Healthy Controls, MCI, Mild Cognitive Impairment; MMSE, Mini Mental State Examination ."+" Indicates that individuals were amyloid positives.

Repeated Measurement ANOVA								
	df	F	$\eta_p^{\ 2}$	p				
Between-subject effects								
Age	1	.335	.003	.564				
Group	2	3.55	.051	.032				
Within-subject effects								
Hemisphere	1	1.34	.010	.249				
$Hemisphere \times Age$	1	1.07	.008	.301				
$Hemisphere \times Group$	2	.162	.002	.850				
Region	1	.272	.002	.603				
Region $\times$ Age	1	.135	.001	.714				
$\textbf{Region} \times \textbf{Group}$	2	3.84	.055	.024				
Hemisphere × Region	1	.949	.007	.332				
Hemisphere $\times$ Region $\times$ Age	1	.950	.007	.332				
$Hemisphere \times Region \times Group$	1	.127	.002	.880				

Table 3. Overall results of the repeated measurement ANOVA, including the factors of group, age, region and hemisphere and their respective interactions. df= degrees of freedom. Bold font indicates significant effects.

Between Group differences	Df	F	p	${\eta_p}^2$
Primary Motor	2	2.11	.125	.031
Area MT, V5	2	2.64	.075	.039535
SMA	2	4.68	.011	.066
Angular Gyrus	2	3.69	.027	$.053^{557}_{538}$
SMG	2	2.54	.083	.037
SPL	2	3.71	.027	.053 <sub>540</sub>
<b>DPMC</b>	2	3.73	.027	.053
Primary Sensory	2	1.17	.331	.017542
Primary Visual	2	1.57	.211	.023
·				5//

Table 4. Summary of the One-Way ANOVA evaluating the group  $\times$  region interaction with the significant main effect of group displayed. The order of regions in this table follows the display order in Figure 2. SMA = supplementary motor area, SMG = supramarginal gyrus, SPL = superior parietal lobe, DPMC = dorsal premotor cortex. Df= degrees of freedom. Regions in bold font show significant effects.

Region	DAD vs.	HC /MCI	Mean Difference (SE)	Significance	Confidence Level lower bound	Confidence Level upper bound	
			(BL)		lower bound		
				SMA			
SMA	DAD	НС	.204 (.067)	.031	.069	.338	
SMA	DAD	MCI	.128 (.055)	.021	.019	.237	
Angular Gyrus							
AG	DAD	НС	.340 (.139)	.015	.064	.617	
AG	DAD	MCI	.280 (.113)	.016	.055	.505	
SPL							
SPL	DAD	НС	.185 (.078)	.021	.028	.340	
SPL	DAD	MCI	.164 (.064)	.012	.037	.290	
DPMC							
DPMC	DAD	НС	.224 (.085)	.010	.055	.393	
DPMC	DAD	MCI	.155 (.069)	.027	.017	.290	

Table 5. Results of the planned post-hoc comparison in regions with a significant group effect (see Table 4); HC = Healthy Controls, MCI = Mild Cognitive Impairment, DAD = Dementia of the Alzheimer's disease type; SE = Standard error, SMA = Supplementary motor area, SMG = Supplementary gyrus, SPL = Superior parietal lobe, DPMC = Supplementary motor cortex.

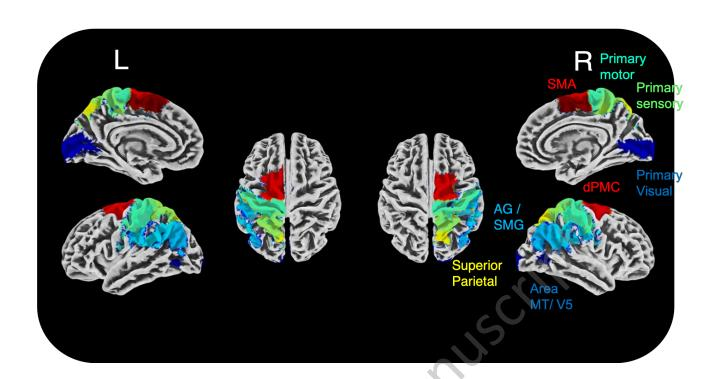
Partial Correlation C (Age, Group)	coefficients		SMA	Angular Gyrus	SPL	DPMC
ADAS-Cog-13	Correlation		.251	.248	.232	.208
	Significance		.004	.004	.007	.017
	df		130	130	130	130
	95% Confidence Interval	Lower	.067	.070	.035	.044
		Upper	.410	.427	.418	.397

Table 6. Partial correlation on relationship between ADAS-Cog-13 and motor regions showing a significant main effect of group on tau SUVR. SMA = supplementary motor area, SPL = superior parietal lobe, DPMC = dorsal premotor cortex. df = degrees of freedom, 95 % confidence interval based on bootstrapping (1000 repetitions) implemented in SPSS v27.

Figure Caption Figure 1. Set of probabilistic regions-of interest (ROIs) used. Cytoarchitectonically regions inferred from the SPM Anatomy toolbox are overlayed on a structural template image in MNI-space using CAT Toolbox. L=left hemisphere, R= right hemisphere, ROIs = Regions of Interest. Colors indicate different label number within the probabilistic motor ROIs, which are exemplary color coded on the right hemisphere. Figure 2. Association of tau pathology in higher-order motor regions with disease category. The mean tau SUVRs for the nine regions are shown collapsed over both hemispheres. The graphs illustrate the significant Region × Group interaction, since a significant group effect for the mean tau SUVRs was observed in four regions (SMA; Supplementary Motor Area, AG; Angular Gyrus, SPL; Superior Parietal Lobe, and DPMC; Dorsal Premotor Cortex), while the tau SUVRs did not differ significantly between the three groups in the other five regions (Primary Motor, Area MT/V5, Supramarginal Gyrus, Primary Sensory, and Primary Visual). HC = Healthy Controls, MCI = Mild Cognitive Impairment, DAD = dementia of the Alzheimer's disease type. \* indicates p<0.05 for the planned post-hoc comparisons *employing t-tests.* Figure 3 Correlation between tau pathology in higher-order motor regions and cognitive dysfunction. Displayed are correlation coefficients from the partial correlation analysis, examining tau pathology in motor regions and performance on the Alzheimer's Disease Assessment Scale-Cognitive Subscale (ADAS-Cog-13) for all participants (n=135). SMA = supplementary motor area. 

- 659 References
- Alahmadi AAS (2021) Investigating the sub-regions of the superior parietal cortex using functional
- magnetic resonance imaging connectivity. Insights into Imaging 12:47.
- Amunts K, Mohlberg H, Bludau S, Zilles K (2020) Julich-Brain: A 3D probabilistic atlas of the human
- brain's cytoarchitecture. Science 369:988–992.
- Bejanin A, Schonhaut DR, La Joie R, Kramer JH, Baker SL, Sosa N, Ayakta N, Cantwell A, Janabi M,
- Lauriola M, O'Neil JP, Gorno-Tempini ML, Miller ZA, Rosen HJ, Miller BL, Jagust WJ, Rabinovici
- 666 GD (2017) Tau pathology and neurodegeneration contribute to cognitive impairment in Alzheimer's
- disease. Brain 140:3286–3300.
- Bischof GN (2022) Tau-PET Bildgebung der Demenzerkrankungen. Angewandte Nuklearmedizin
- 669 45:266–272.
- Bischof GN, Endepols H, van Eimeren T, Drzezga A (2017) Tau-imaging in neurodegeneration.
- 671 Methods 130:114–123.
- Braak H, Braak E (1995) Staging of Alzheimer's disease-related neurofibrillary changes.
- Neurobiology of aging 16:271–278; discussion 278-84.
- Braak H, Thal DR, Ghebremedhin E, Del Tredici K (2011) Stages of the pathologic process in
- Alzheimer disease: age categories from 1 to 100 years. J Neuropathol Exp Neurol 70:960–969.
- 676 Côté SL, Elgbeili G, Quessy S, Dancause N (2020) Modulatory effects of the supplementary motor
- area on primary motor cortex outputs. J Neurophysiol 123:407–419.
- Del Tredici K, Braak H (2020) To stage, or not to stage. Current Opinion in Neurobiology 61:10–22.
- Dronse J, Fliessbach K, Bischof GN, von Reutern B, Faber J, Hammes J, Kuhnert G, Neumaier B,
- Onur OA, Kukolja J, van Eimeren T, Jessen F, Fink GR, Klockgether T, Drzezga A (2016) In vivo
- 681 Patterns of Tau Pathology, Amyloid-β Burden, and Neuronal Dysfunction in Clinical Variants of
- Alzheimer's Disease. J Alzheimers Dis 55:465–471.
- Eickhoff SB, Stephan KE, Mohlberg H, Grefkes C, Fink GR, Amunts K, Zilles K (2005) A new SPM
- toolbox for combining probabilistic cytoarchitectonic maps and functional imaging data. NeuroImage
- 685 25:1325–1335.
- 686 Gonzalez-Escamilla G, Lange C, Teipel S, Buchert R, Grothe MJ, Alzheimer's Disease Neuroimaging
- 687 Initiative (2017) PETPVE12: an SPM toolbox for Partial Volume Effects correction in brain PET -
- Application to amyloid imaging with AV45-PET. Neuroimage 147:669–677.
- 689 Grothe MJ, Barthel H, Sepulcre J, Dyrba M, Sabri O, Teipel SJ, Alzheimer's Disease Neuroimaging
- 690 Initiative (2017) In vivo staging of regional amyloid deposition. Neurology 89:2031–2038.
- Horwitz B, Rumsey JM, Donohue BC (1998) Functional connectivity of the angular gyrus in normal
- reading and dyslexia. Proceedings of the National Academy of Sciences 95:8939–8944.
- Jack CR, Wiste HJ, Schwarz CG, Lowe VJ, Senjem ML, Vemuri P, Weigand SD, Therneau TM,
- Knopman DS, Gunter JL, Jones DT, Graff-Radford J, Kantarci K, Roberts RO, Mielke MM, Machulda
- 695 MM, Petersen RC (2018) Longitudinal tau PET in ageing and Alzheimer's disease. Brain 141:1517–
- 696 1528.
- 697 Johnen A, Tokaj A, Kirschner A, Wiendl H, Lueg G, Duning T, Lohmann H (2015) Apraxia profile
- 698 differentiates behavioural variant frontotemporal from Alzheimer's dementia in mild disease stages. J
- 699 Neurol Neurosurg Psychiatry 86:809–815.

- Klein AP, Ulmer JL, Quinet SA, Mathews V, Mark LP (2016) Nonmotor Functions of the Cerebellum:
- An Introduction. American Journal of Neuroradiology 37:1005–1009.
- Leuzy A, Chiotis K, Lemoine L, Gillberg P-G, Almkvist O, Rodriguez-Vieitez E, Nordberg A (2019)
- Tau PET imaging in neurodegenerative tauopathies-still a challenge. Mol Psychiatry.
- Martin M, Hermsdörfer J, Bohlhalter S, Weiss PH (2017) [Networks involved in motor cognition :
- Physiology and pathophysiology of apraxia]. Nervenarzt 88:858–865.
- McKhann G, Drachman D, Folstein M, Katzman R, Price D, Stadlan EM (1984) Clinical diagnosis of
- Alzheimer's disease: report of the NINCDS-ADRDA Work Group under the auspices of Department
- of Health and Human Services Task Force on Alzheimer's Disease. Neurology 34:939–944.
- 709 Murray ME, Lowe VJ, Graff-Radford NR, Liesinger AM, Cannon A, Przybelski SA, Rawal B, Parisi
- JE, Petersen RC, Kantarci K, Ross OA, Duara R, Knopman DS, Jack CR, Dickson DW (2015)
- 711 Clinicopathologic and 11C-Pittsburgh compound B implications of Thal amyloid phase across the
- 712 Alzheimer's disease spectrum. Brain 138:1370–1381.
- 713 Mutha PK, Haaland KY, Sainburg RL (2012) THE EFFECTS OF BRAIN LATERALIZATION ON
- 714 MOTOR CONTROL AND ADAPTATION. J Mot Behav 44:455–469.
- Ossenkoppele R et al. (2016) Tau PET patterns mirror clinical and neuroanatomical variability in
- 716 Alzheimer's disease. Brain 139:1551–1567.
- Rahimpour S, Rajkumar S, Hallett M (2022) The Supplementary Motor Complex in Parkinson's
- 718 Disease. J Mov Disord 15:21–32.
- 719 Schöll M, Lockhart SN, Schonhaut DR, O'Neil JP, Janabi M, Ossenkoppele R, Baker SL, Vogel JW,
- 720 Faria J, Schwimmer HD, Rabinovici GD, Jagust WJ (2016) PET Imaging of Tau Deposition in the
- 721 Aging Human Brain. Neuron 89:971–982.
- 722 Schwarz AJ, Yu P, Miller BB, Shcherbinin S, Dickson J, Navitsky M, Joshi AD, Devous MD Sr,
- 723 Mintun MS (2016) Regional profiles of the candidate tau PET ligand 18F-AV-1451 recapitulate key
- features of Braak histopathological stages. Brain: a journal of neurology 139:1539–1550.
- 725 Tanji J (1994) The supplementary motor area in the cerebral cortex. Neurosci Res 19:251–268.
- 726 Tanji J, Shima K (1996) Supplementary motor cortex in organization of movement. Eur Neurol 36
- 727 Suppl 1:13–19.
- 728 Thal DR, Rüb U, Orantes M, Braak H (2002) Phases of A beta-deposition in the human brain and its
- relevance for the development of AD. Neurology 58:1791–1800.
- Vogel JW, Young AL, Oxtoby NP, Smith R, Ossenkoppele R, Strandberg OT, La Joie R, Aksman
- LM, Grothe MJ, Iturria-Medina Y, Alzheimer's Disease Neuroimaging Initiative, Pontecorvo MJ,
- Devous MD, Rabinovici GD, Alexander DC, Lyoo CH, Evans AC, Hansson O (2021) Four distinct
- trajectories of tau deposition identified in Alzheimer's disease. Nat Med 27:871–881.
- Wren MC, Lashley T, Årstad E, Sander K (2018) Large inter- and intra-case variability of first
- 735 generation tau PET ligand binding in neurodegenerative dementias. Acta Neuropathologica
- 736 Communications 6:34.
- 737 Yliranta A, Karjalainen V-L, Nuorva J, Ahmasalo R, Jehkonen M (2023a) Apraxia testing to
- distinguish early Alzheimer's disease from psychiatric causes of cognitive impairment. Clin
- 739 Neuropsychol:1–22.
- 740 Yliranta A, Nuorva J, Karjalainen V-L, Ahmasalo R, Jehkonen M (2023b) The dementia apraxia test
- can detect early-onset Alzheimer's disease. Neuropsychology 37:44–51.



e Meuro Accepted Mark

